

3 THE ROLE OF MOISTURE AND HYDROGEN IN  
HOT-SALT CRACKING OF TITANIUM ALLOYS

by

S. P. Rideout, R. S. Ondrejcin,

M. R. Louthan, Jr., and D. E. Rawl

Savannah River Laboratory

E. I. du Pont de Nemours and Company

Aiken, South Carolina, 29801

A.E.C.  
R-124

GPO PRICE \$

CSFTI PRICE(S) \$

Hard copy (HC) 3.00

Microfiche (MF) .65

4511672

ff 653 July 65

FACILITY FORM 602	N 68-34204	
	(ACCESSION NUMBER)	(THRU)
	41	1
	(PAGES)	(CODE)
	CR-89805	17
	(NASA CR OR TMX OR AD NUMBER)	(CATEGORY)

15 Submitted  
for publication

## I. ABSTRACT

The role of moisture and hydrogen in the stress corrosion cracking of Ti-8Al-1Mo-1V exposed to hot chloride salts was investigated. The adsorption and retention of moisture during the application of salt deposits and subsequent heating, and the extent of HCl and hydrogen generation during corrosion were studied using radiotracer techniques and mass spectrographic analyses of volatile corrosion products. Hot-stage microscopy and cinematography were used to study crack initiation and propagation, and the characteristics of fracture surfaces were examined by electron fractography. The effects of NaCl were compared to those of  $\text{SnCl}_2 \cdot 2\text{H}_2\text{O}$ , which not only retains much more moisture but also has a much lower melting point than NaCl. These studies revealed an obvious association between the occurrence of cracking and the amounts of HCl and hydrogen generated during hot-salt corrosion. This, combined with results of supplementary experiments using sodium iodide and bromide, indicates that hydrogen, rather than the halide, plays the key role in the cracking process. The observations are consistent with a stress-sorption mechanism for cracking, in which corrosion-produced nascent hydrogen is proposed to be the sorbed species responsible for cracking.

## II. INTRODUCTION

Information concerning the susceptibility of titanium alloys to stress corrosion cracking has accumulated rapidly during recent years as a result of extensive laboratory testing programs to evaluate high-strength engineering materials for aircraft, space, and marine applications. The first cause for concern that susceptibility to stress corrosion might be a significant problem in the use of titanium alloys was the discovery that some alloys crack when stressed in contact with chloride salts at elevated temperatures.<sup>(1,2)</sup> This phenomenon, called hot-salt cracking, is a threat to many titanium alloy structural components operating at elevated temperature because sources of chloride contamination are so numerous. The list of other environments that can produce stress corrosion damage in titanium alloys has grown since 1964, when it was discovered that specimens with pre-existing fatigue cracks are susceptible to stress corrosion at room temperature in sea water.<sup>(3)</sup> Cracking can occur at ambient temperatures in a variety of aqueous and nonaqueous media. Many laboratories currently are investigating the mechanism of cracking in various environments. The Savannah River Laboratory, under sponsorship of the National Aeronautics and Space Administration, is conducting research to develop fundamental information on the phenomenon of hot-salt cracking.

Hot-salt cracking was first thought to be caused by dry salt deposits, and moisture was not considered to be important.<sup>(2)</sup> Chlorine gas, produced as an intermediate and regenerable product of salt-metal reactions in the presence of oxygen or a reducible oxide, was proposed to be the cause of stress corrosion. However, this proposal was based on observations of hot-salt corrosion effects at test temperatures from 900° to 1400°F<sup>(2)</sup> and on analytical evidence of small amounts of chlorine in volatile products of corrosion at 1200°F.<sup>(4)</sup>

In contrast, studies at SRL<sup>(5)</sup> on NaCl cracking of Ti-8Al-1Mo-1V at a lower temperature (650°F) indicated that moisture is important in the salt corrosion process, and that HCl gas is generated. Exposure of stressed specimens to hot HCl gas alone, with no salt deposit, caused cracking which occurred in a manner similar to the delayed failure phenomenon associated with hydrogen embrittlement. Several features of the hot-salt cracking phenomenon also indicated that corrosion-produced hydrogen might be involved in the mechanism of cracking. Through the use of radiotracer techniques,<sup>(5)</sup> hydrogen was shown to be retained in areas corroded at 650°F by salt initially deposited from a solution containing tritiated water,  $^3\text{H}_2\text{O}$ . Direct, hot-stage metallographic observations of hot-salt stress corrosion revealed that cracks initiated abruptly following an incubation period, the duration of which depended on exposure temperature, salt

composition, and alloy composition.<sup>(6)</sup> The effect of salt composition on the incubation period for cracking was also investigated, particularly with respect to the amounts of moisture retained in the salt deposit and the amounts of HCl gas and hydrogen generated during corrosion.<sup>(7)</sup> Those results were the basis for the proposal that corrosion-produced hydrogen rather than chlorine gas is responsible for hot-salt cracking.

The objective of this paper is to further define how moisture, HCl, and hydrogen are involved in hot-salt stress corrosion of titanium alloys.

### III. EXPERIMENTAL PROCEDURES

#### A. Specimens for Radiotracer Studies and Hot-Stage Microscopy

As described for previous studies<sup>(7)</sup> the test specimens were metallographically polished 3/4- x 3- x 0.050-inch strips of duplex-annealed Ti-8Al-1Mo-1V alloy. The strips were mounted in 4-point loading holders and stressed by bending to a surface-fiber stress of  $10^5$  psi at room temperature, which caused them to yield slightly when heated to test temperatures.

Salt solutions used in studies of adsorption of moisture and chlorides (Tables I-IV) were made radioactive by adding either tritium as  $^3\text{H}_2\text{O}$  (1 Ci per ml)  $^{22}\text{NaCl}$  (1 Ci per ml) or chloride as  $\text{Na}^{36}\text{Cl}$  (0.03 mCi per ml). The presence of tritium on the specimens was determined by counting in a windowless, gas-flow proportional counter, and the chloride was counted with a GM beta counter. The absorption of hydrogen (as  $^3\text{H}$ ) by the metal in salt-corroded areas was confirmed by first removing all salt, etching the surface to dissolve a small increment of metal, and then counting the etching solution in a beta liquid scintillation counter.

For experiments to determine the time to initiate cracking, (Table V) deposits of salt were applied in the area of maximum stress by evaporating three drops of saturated aqueous solution on the specimens. This procedure produced a fairly dense deposit of coarse

crystals covering a spot about 1/2 inch in diameter. Multiple specimens were then heated isothermally in stagnant air using a small electric oven. Specimens were removed at intervals, and after removing the salt deposits, the surfaces were microscopically examined for evidence of cracking.

In order to permit direct hot-stage metallographic observations of salt-metal reactions, droplets of dilute solutions were evaporated on the pre-polished surfaces.<sup>(6)</sup> The resultant salt crystals were small enough to be viewed with a conventional metallurgical microscope. The specimen loading fixture was positioned directly on the microscope stage, and heating was accomplished by placing a tiny, hand-made coil of resistance wire against the underside of the specimen and adjusting the current with a powerstat. Movies of the hot-salt stress corrosion process were made through the eyepiece of the microscope using a 16-mm camera equipped with a single frame attachment for speeds down to one frame per second.

The characteristics of stress corrosion fracture surfaces were studied by conventional replication and electron microscopy techniques.

#### B. Mass Spectrometer Analyses of Volatile Corrosion Products

A Consolidated Engineering Corp. Model 21-103 mass spectrometer was used to analyze volatile corrosion products that were evolved when mixtures of Ti-8Al-1Mo-1V alloy and sodium chloride

were heated in a closed, heated glass reaction vessel attached directly to the mass spectrometer.<sup>(7)</sup> Titanium alloy chips were wetted with salt solution and dried for 1 hour at 110°C. Chips were used to assure a high surface area/salt ratio. The pressure in the reaction vessel was reduced so that at temperature, without a reaction, the pressure would be 1 atmosphere. About 2% of the gas in the reaction vessel was removed each time a sample was taken. The stopcocks in the reaction vessel and on the mass spectrometer were greased with "Kel-F,"\* a lubricant unattacked by Cl<sub>2</sub> and other strong oxidants.

#### C. Electron Microprobe Analyses

The distribution of Na and Cl in cracks and adjacent regions was determined using a Materials Analysis Corporation Model 400 electron microprobe.<sup>(7)</sup> X-rays were diffracted with a potassium acid phthalate crystal for Na and a pentaerythritol crystal for Cl. Spectrometers were calibrated with carbon-coated sodium chloride crystals, so that atomic concentrations of Na and Cl could be shown on equivalent scales in Figure 7.



#### IV. RESULTS AND DISCUSSION

##### A. Radiotracer Studies of Adsorption

Previous work<sup>(5)</sup> showed that some form of chloride other than NaCl is strongly adsorbed on titanium alloy surfaces that are wetted at room temperature with NaCl solution and subsequently rinsed in flowing hot water. Continuation of the adsorption studies<sup>(7)</sup> showed preferential adsorption of chlorides on a variety of metals, Table I. The effect of solution pH on chloride adsorption by Ti-8Al-1Mo-1V at room temperature, Figure 1, indicates that the chloride is not present as HCl molecules, because the absorption was maximum in the pH 5-6 range and decreased as the pH was increased or decreased. If adsorbed chloride ions were accompanied by hydrogen ions, the amount adsorbed would be expected to increase in acidic solutions. Based on the results of these studies, it is proposed that chloride ions are absorbed into the metal oxide film, probably occupying oxygen vacancies in the lattice. The presence of chloride ions in the oxide film should contribute to the breakdown of passivity during exposure at elevated temperatures.

Because chloride absorption at room temperature was not associated with hydrogen ions or HCl molecules, the HCl gas detected during hot-salt corrosion must be generated by reactions involving moisture. Various possible sources of moisture were investigated as described below.

Experiments with radiotracer  $^3\text{H}$ , as  $^3\text{H}_2\text{O}$ , Figure 2, demonstrated that moisture is adsorbed on titanium alloy surfaces that appear to be dry at room temperature. In these tests, specimens with and without prior exposure to NaCl solution were wetted with  $^3\text{H}_2\text{O}$  and allowed to dry at room temperature. In Figure 2 both specimens showed a gradual decrease in radioactivity during aging at room temperature, which would be expected due to an exchange between atmospheric and adsorbed moisture. Prior exposure to NaCl solution had no significant effect on moisture adsorption; the slight difference shown in Figure 2 is within the range of reproducibility on duplicate specimens.

On specimens that were dried in air immediately after wetting, the  $^3\text{H}_2\text{O}$  was easily removed by exchange with hot rinse water, indicating that the moisture was not tightly bound to the surface. On specimens immersed for extended times in tritiated salt solutions, the hot water rinse did not remove all of the radiotracer, Table II. This retention may be due to absorption of some moisture into the oxide film.

In order to demonstrate that the most important source of moisture involved in hot-salt corrosion is that which is retained in salt deposited by evaporation of solutions, deposits of

NaCl and  $\text{SnCl}_2 \cdot 2\text{H}_2\text{O}$  containing tritium traces were studied (Table III). The amount of moisture adsorbed in the salt deposit was significantly greater than the amount retained by the absorption in the protective oxide film (Figure 2).

The effect of retained moisture on stress corrosion cracking was compared on specimens with pre-dried salt crystals, Figure 3.<sup>(7)</sup> The Ti-8Al-1Mo-1V specimens were photographed directly through the hot-stage microscope after being heated at 650°F for 90 minutes. Corrosion staining and cracking occurred in the sequence reported previously<sup>(6)</sup> on the specimen with the "moist" salt; but there was no evidence of corrosion or cracking on the specimen exposed to the predried salt crystals. Under these test conditions, neither moisture present in room air nor moisture adsorbed on the specimen surface were sufficient to initiate stress-corrosion. The possibility remains, however, that atmospheric moisture might be sufficient to promote attack after much longer exposure times or after exposure at higher temperatures.

After heating a specimen at 650°F for 75 hours and subsequently cooling and removing all salt and corrosion products from the surface, the absorption of corrosion-produced hydrogen by the metal was shown by counting the  $^3\text{H}$  activity, Table IV. The data substantiates the observation of  $^3\text{H}$  in salt-corroded areas made previously<sup>(5)</sup> by autoradiographic techniques.

## B. Effect of Type of Salt and Moisture Content on Cracking

In previous studies,<sup>(6,7)</sup> the time to initiate hot-salt cracking was shown to be dependent on exposure temperature, salt composition, and alloy composition. In a continuation of these studies, the effect of moisture content of the salt on cracking of Ti-8Al-1Mo-1V was investigated by comparing the effects of NaCl with  $\text{SnCl}_2 \cdot 2\text{H}_2\text{O}$ . As shown in Figure 4, the time to initiate cracking was much shorter for  $\text{SnCl}_2 \cdot 2\text{H}_2\text{O}$  than for NaCl, especially at temperatures above the melting point of  $\text{SnCl}_2$ , 475°F. Although the liquid salt greatly accelerates the stress corrosion phenomenon, it is important to note that cracking can occur at temperatures below the melting points of both  $\text{SnCl}_2$  and NaCl. This indicates that the presence of a liquid phase is not an essential requirement for hot-salt cracking.

The electrochemical nature of hot-salt corrosion reactions was vividly revealed by the experiments performed at temperatures above the melting point of  $\text{SnCl}_2$ . During the initial attack by the fused salt, small globules of pure, molten tin appeared on the specimens. This tin metal, the identity of which was confirmed by chemical analysis, could only be produced by electrochemical oxidation of the titanium alloy specimen and reduction of the tin ions ( $\text{Sn}^{++}$ ) of the salt to tin metal. The oxidation of the titanium

alloy was obvious from the formation of corrosion pits. During continued exposure to the atmosphere, the tin metal oxidized. Cracking was initiated only after significant corrosion had occurred, which indicates that the cracking was not caused by the liquid tin, or by titanium corrosion products (such as titanium chlorides). This was confirmed by immersing stressed Ti-8Al-1Mo-1V in molten tin at 700°F, abrading the surface to break the oxide film, and exposing it for 90 minutes. No cracking occurred.

Evidence in support of a stress-sorption theory of cracking was found during the hot-stage microscopy experiments. Hot-stage microscopy revealed that, with both NaCl and  $\text{SnCl}_2 \cdot 2\text{H}_2\text{O}$ , the initial propagation of cracks was very rapid. However, cracks caused by NaCl were small, and further growth occurred very slowly, apparently by intermittent extensions. Cracking caused by  $\text{SnCl}_2 \cdot 2\text{H}_2\text{O}$  was much more severe, and the initial extent of cracking was directly dependent on the amount of salt on the specimen. The addition of more  $\text{SnCl}_2 \cdot 2\text{H}_2\text{O}$  to hot specimens caused immediate rapid extension of cracks. In some cases in which the specimens were cooled to room temperature after the initial cracks formed, the residual salt and corrosion products partially dissolved as a result of absorbing atmospheric moisture, and further rapid crack propagation (0.1 inch/min) was observed at room temperature. This behavior appears to be

similar to the stress corrosion that has been reported<sup>(3)</sup> in titanium alloys precracked by fatigue and exposed to ambient temperature corrosion media. The rapid crack propagation at room temperature appear to be best explained on the basis of a stress-sorption mechanism of cracking.

Evidence of "tunneling," i.e., lateral extension of the crack beneath the specimen surface was observed, especially in the case of  $\text{SnCl}_2$  cracking. An obvious example is illustrated in Figure 5, which shows the ends of cracks extending through to the edge of a specimen before they extended the full width of the specimen. Figure 5 also shows plastic deformation and "necking" ahead of the advancing cracks.

#### C. Analyses of Volatile Corrosion Products

The difference in cracking severity caused by  $\text{NaCl}$  and  $\text{SnCl}_2 \cdot 2\text{H}_2\text{O}$  appears to be due to the greater amount of moisture, and consequently the greater quantities of  $\text{HCl}$  and hydrogen generated during corrosion by  $\text{SnCl}_2 \cdot 2\text{H}_2\text{O}$ , as shown in Figure 6.

These mass spectrochemical analyses of volatile corrosion products generated during attack of  $\text{Ti-8Al-1Mo-1V}$  by the two different salts show an obvious association with the time to initiate cracking, Figure 4, and the relative amounts of  $\text{HCl}$  and hydrogen produced, Figure 6. At  $500^\circ\text{F}$ , more than 10,000 times as

much HCl and hydrogen were generated by  $\text{SnCl}_2 \cdot 2\text{H}_2\text{O}$  than by NaCl, and within much shorter times.

The marked increase in the concentration of hydrogen during the initial periods of corrosion, Figure 6, supports the hypothesis that corrosion-produced hydrogen promotes cracking. No chlorine gas was detected in the volatile corrosion products. Spectral data were collected to mass 170 to ensure that  $\text{TiCl}_2$  or  $\text{TiCl}_3$  would be detected if present. However, only  $\text{H}_2\text{O}$ , HCl, and  $\text{H}_2$  were observed as volatile corrosion products. The metal chlorides were not expected because they should hydrolyze in air at the exposure temperature to produce oxides, HCl, and hydrogen.

The production of halogen acids by the reaction of water with a hydrolyzable halide salt at elevated temperature is termed pyrohydrolysis and is a common analytical technique for the analysis of halide salts.<sup>(8)</sup> Pyrohydrolysis requires a reaction of  $\text{H}_2\text{O}$  with the halide salt to form a volatile species of the halogen (e.g., HCl, HBr). This reaction is often accelerated by the addition of aluminum oxide or vanadium pentoxide when the salt is difficult to hydrolyze, as is the case with NaCl. Thus, previous reports<sup>(2,4)</sup> that metal oxides are involved in hot-salt cracking can be explained on the basis that the oxide accelerates pyrohydrolysis. In some cases, water of hydration in metal oxides would also contribute to the process.

All of the ingredients for pyrohydrolysis are present in the hot-salt stress corrosion of titanium alloys.<sup>(7)</sup> Both aluminum and vanadium are present in the oxide film on Ti-8Al-1Mo-1V alloy; HCl has been observed as a corrosion product, and water has been shown to be necessary for hot-salt cracking. Thus, the experimental evidence demonstrates that pyrohydrolysis initiates the corrosion process. HCl penetration of the oxide film, rendered less protective by the prior absorption of chloride, produces attack of the metal to form metal chlorides and hydrogen. More HCl and hydrogen are then generated by hydrolysis of the metal chlorides.

Evidence that HCl, rather than NaCl is the form of chloride present in cracks was obtained by electron microprobe analyses for Na and Cl along the length of cracks.<sup>(7)</sup> Specimens that were cracked during exposures to NaCl at 650°F were polished in nonaqueous lubricants so that the crack cross section could be scanned by an expanded, 8μ diameter electron beam. Care was taken to prevent sodium chloride from being forced into the crack during sample preparation. Seven cracks were examined. Crack depth ranged from 75μ to 320μ. These analyses showed that sodium was concentrated at the mouth of the crack and that chloride was present in decreasing concentrations from the mouth toward the crack tip. A typical crack and the accompanying sodium and chloride concentration profiles are



shown in Figure 7. The penetration of chloride but not sodium was also supported by autoradiographic studies<sup>(7)</sup> of samples cracked with  $^{22}\text{NaCl}$  and  $\text{Na}^{36}\text{Cl}$ . The chloride tracer but not sodium was found concentrated in the cracked regions.

#### D. Electron Microscopy of Stress Corrosion Crack Surfaces

Examinations of the fracture surfaces of Ti-8Al-1Mo-1V alloy samples cracked by exposure to moist and dry HCl,  $\text{SnCl}_2 \cdot 2\text{H}_2\text{O}$ , and NaCl revealed that cracking in all cases was predominately intergranular with limited regions of transgranular cleavage. Little evidence of ductile failure was noted. In general, the observations were consistent with a stress-sorption mechanism of fracture. Evidence of dislocation movement, and therefore plastic deformation accompanying fracture was also observed. Some evidence of corrosion on fracture surfaces was observed but corrosion probably occurred after the fracture was formed.

Typical fractographs of samples cracked under five different conditions are shown in Figure 8. The fracture surfaces are quite similar and several features are common to most of the samples:

- A. Intergranular cracking, shown by grain shapes is revealed on the fracture surface. There was little evidence of ductile failure.
- B. Secondary cracking.

C. Rough grain surfaces with areas of more or less regular ripples, steps or folds (see arrows). These regions probably result from serpentine glide, glide plane decohesion and stretching, and are interpreted as evidence of dislocation movement during the formation of the fracture surfaces. Figure 9 shows such regions in more detail.

D. Pitting, probably resulting from corrosion after cracking was also observed in some samples (compare Figures 8a, b, and c with d and e). Severely pitted regions are shown in Figure 10 to emphasize the extent to which corrosion can occur.

The river patterns, Figure 11, characteristic of transgranular cleavage were observed in limited regions of most of the samples. The relatively smooth grain surfaces, the topographic features, and the evidence of cleavage fracture indicate that failure must have been mechanical although electrochemical corrosion occurred at the surface. Thus, the most reasonable mechanism for hot-salt cracking appears to be the stress-sorption mechanism.

#### E. Cracking in Various Halide Salts

Previous work<sup>(5-7)</sup> demonstrated that various halide salts in addition to NaCl can cause hot-salt cracking of titanium alloys.

The times required for crack initiation in Ti-8Al-1Mo-1V exposed to various halide salts deposited from saturated solutions are shown in Table V. The effectiveness of the halide in promoting cracking increased as the size of the ion decreased (i.e.,  $\text{Cl} > \text{Br} > \text{I}$ ). The pH of the saturated salt solution initially applied to the specimen is also important; the time to initiate cracking decreased with decreasing pH, Table V. This result indicates that the hydrogen ion is more important than the halide ion in promoting cracking.

## V. CONCLUSIONS

The principal experimental results to date that support a stress-sorption mechanism for hot-salt cracking of titanium alloys are;

- o Surface corrosion products are generated prior to cracking
- o Cracking is due to mechanical fracture with corrosion after propagation
- o After initiation, rapid crack propagation occurs, even at room temperature.

Of the two species, hydrogen chloride and hydrogen, that might be active in the stress sorbtion process, corrosion-produced nascent hydrogen is proposed to be the sorbed species responsible for cracking. The stress corrosion cracking process appears to occur by the following sequence:

- a. Moisture retained in salt deposits is required to initiate pyrohydrolysis of the salt in contact with the metal oxide film.
- b. Pyrohydrolysis generates a hydrogen halide, which penetrates the oxide film and reacts to form metal halides and hydrogen.
- c. Hydrolysis of the metal halides reforms a hydrogen halide and generates hydrogen.
- d. Hydrogen is sorbed by the metal surface, weakens the inter-metallic bonds, and causes cracks to form because of the applied stress.

# FOOTNOTES

Page 1 - The Savannah River Laboratory is operated by the E. I. du Pont de Nemours and Company for the U. S. Atomic Energy Commission, under Contract AT(07-2)-1. The work reported here was done for the National Aeronautical Space Administration, under ~~Purchase~~ Order R-124 issued to the USAEC.

Page 8 - Trademark of Minnesota Mining and Manufacturing Company, St. Paul, Minnesota.

## VI. REFERENCES

1. G. W. Bauer, "Elevated Temperature Stability of Commercial Titanium Alloys." Paper presented at Physical Metallurgy Symposium, Watertown Arsenal (September 1955).
2. Progress Report on the Salt Corrosion of Titanium Alloys at Elevated Temperature and Stress, TML Report No. 88, (November 1957).
3. B. F. Brown, "A New Stress-Corrosion Cracking Test Procedure for High-Strength Alloys," Materials Research and Standards, Vol. 6, No. 3, (March 1966).
4. V. C. Petersen and H. B. Bomberger, "The Mechanism of Salt Attack on Titanium Alloys," Stress-Corrosion Cracking of Titanium, ASTM STP 397, (1966) pp. 80-94.
5. S. P. Rideout, M. R. Louthan, Jr., and C. L. Selby, "Basic Mechanisms of Stress-Corrosion Cracking of Titanium," Stress Corrosion Cracking of Titanium, ASTM STP 397, (1966) pp. 137-151.
6. S. P. Rideout, "The Initiation of Hot-Salt Stress Corrosion Cracking of Titanium Alloys." Paper presented at the ASTM Symposium on Applications-Related Phenomena in Titanium Alloys, Los Angeles, California (April 1967); to be published in an ASTM Special Technical Publication.

7. R. S. Ondrejcin, C. L. Selby, and S. P. Rideout, Role of Chloride in Hot-Salt Stress-Corrosion Cracking of Titanium-Aluminum Alloys, USAEC Report DP(NASA)-1118 (July 1967).
8. C. J. Rodden, "Analytical Chemistry of the Manhattan Project," McGraw-Hill Book Co., New York (1950) p. 729.

Table I

Adsorption of  $\text{Na}^+$  and  $\text{Cl}^-$  on Selected Metals (a) (7)

<u>Material</u>	<u>Surface Condition</u>	<u>Adsorption, <math>\mu\text{g}/10 \text{ cm}^2</math></u>	
		<u><math>\text{Na}^+</math></u>	<u><math>\text{Cl}^-</math></u>
Type 304 Stainless Steel	Polished	0.00	12.0
Titanium	Polished	0.00	12.0
Ti-8Al-1Mo-1V	Polished	0.14	10.0
Ti-8Al-1Mo-1V	Mill Oxide	0.03	9.4
Tantalum	Oxidized	0.01	10.0
Zircaloy-2	Oxidized	0.03	8.5
Platinum	Oxidized	0.00	4.5

(a)  $\text{Na}^+$  as radiotracer  $^{22}\text{Na}$

$\text{Cl}^-$  as radiotracer  $^{36}\text{Cl}$



Table II

Effect of Immersion Time of Ti-8Al-1Mo-1V on

Adsorption of  $^3\text{H}_2\text{O}$  from NaCl Solution (pH 6.0)

Specimen	Immersion	Treatment After	Counts/10 min	
<u>No.</u>	<u>Time, hr</u>	<u>Immersion</u>	<u>(3.6 cm<sup>2</sup> surface area)</u>	
			Counter	2 $\sigma$
			<u>Reading</u>	<u>Error</u>
1	0.5	Dried with absorbent tissue in air	534	$\pm 240$
2	0.5	(Same as above)	725	$\pm 240$
		Subsequently rinsed in flowing hot water	190	$\pm 240$
3	0.5	Dried with absorbent tissue and rinsed immediately in flowing hot water	31	$\pm 240$
4	26	Dried with absorbent tissue	1130	$\pm 260$
5	26	(Same as above)	862	$\pm 260$
		Subsequently rinsed in flowing hot water	699	$\pm 260$
6	26	Dried with absorbent tissue and rinsed immediately in flow- ing hot water	519	$\pm 260$

Table III

$^3\text{H}_2\text{O}$  Radiotracer Indication  
of Moisture in Salt Deposits

<u>Type of Salt Deposit(a)</u>	<u>Counts per Minute</u>
NaCl	35,600
$\text{SnCl}_2 \cdot 2\text{H}_2\text{O}$	149,400

(a) Produced by evaporation of 100  $\mu\text{l}$  of saturated  
salt solution of Ti-8Al-1Mo-1V specimen.

Table IV

Hydrogen ( $^3\text{H}$ ) Absorption by Ti-8Al-1Mo-1V

in Salt-Corroded Area

<u>Specimen No.</u>	<u><math>\beta</math> Counter Reading, Counts/10 min</u>			<u><math>2\sigma</math> Error</u>	
	<u>Specimen Treatment</u> <sup>(a)</sup>	<u>A</u>	<u>B</u>	<u>C</u>	
1		1461	430	0	$\pm 245$
2		1069	352	325	$\pm 245$

(a) Specimen Treatment: Stressed Specimens treated with hot NaCl for 75 hours at  $650^\circ\text{F}$  and rinsed in flowing hot water for one minute.

A - Counts made after two chemical etches that removed a total 0.2 mil.

B - Counts made after an additional 0.1 mil removed by grinding.

C - Counts made after an additional 0.1 mil removed by grinding.

Table V  
Effects of Type of Halogen Salt and  
Initial Solution pH on Time to Initiate  
Cracking of Ti-8Al-1Mo-1V<sup>(7)</sup>

<u>Salt</u>	pH of	Exposure	Time to Initiate
	Initial Solution	Temp, °F	Cracking, min
NaCl	4.1	650	80
	0.5	650	40
NaBr	4.7	650	150
	0.5	650	75
NaI	8.9	750	150
	0.5	750	75
SnCl <sub>2</sub> ·2H <sub>2</sub> O	4.1	650	30
	0.5	650	15
	0.2	650	10
CuCl	3.4	650	60

## FIGURE CAPTIONS

- Figure 1. Effect of pH on Adsorption of  $\text{Cl}^-$  by Ti-8Al-1Mo-1V in NaCl Solutions<sup>(7)</sup>
- Figure 2. Radiotracer Evidence of Adsorbed Moisture (or  $^3\text{H}_2\text{O}$ ) on Ti-8Al-1Mo-1V at Room Temperature
- Figure 3. Effect of Moisture on NaCl Cracking of Ti-8Al-1Mo-1V at 650°F<sup>(7)</sup> (Specimen was exposed 90 minutes)
- Figure 4. Effects of Salt Composition and Temperature on Time to Initiate Cracking of Ti-8Al-1Mo-1V
- Figure 5. "Tunneling" of  $\text{SnCl}_2$ -Induced Cracks in Ti-8Al-1Mo-1V (Specimen was exposed at 650°F for 10 min.)
- Figure 6. Evolution of  $\text{H}_2$  and HCl During Hot Salt Corrosion of Ti-8Al-1Mo-1V
- Figure 7. Electron Microprobe Analyses of Na and Cl in Hot-Salt Crack in Ti-8Al-1Mo-1V<sup>(7)</sup>
- Figure 8. Typical Fractographs of Hot-Salt Cracks in Ti-8Al-1Mo-1V
- Figure 9. Fractographs Showing Evidence of Dislocation Movement Accompanying Fracture During Hot-Salt Cracking
- Figure 10. Fractographs Showing Evidence of Corrosion of Fracture Faces
- Figure 11. Fractograph Showing Typical River Patterns Found in Limited Regions of Both Hot-Salt and HCl Cracks

## TABLE OF CONTENTS

	<u>Page</u>
I. ABSTRACT . . . . .	2
II. INTRODUCTION . . . . .	3
III. EXPERIMENTAL PROCEDURES . . . . .	6
A. Specimens for Radiotracer Studies and Hot- Stage Microscopy . . . . .	6
B. Mass Spectrometer Analyses of Volatile Corrosion Products . . . . .	7
C. Electron Microprobe Analyses . . . . .	8
IV. RESULTS AND DISCUSSION . . . . .	9
A. Radiotracer Studies of Adsorption . . . . .	9
B. Effect of Type of Salt and Moisture Content on Cracking . . . . .	12
C. Analyses of Volatile Corrosion Products . . . . .	14
D. Electron Microscopy of Stress Corrosion Crack Surfaces . . . . .	17
E. Cracking in Various Halide Salts . . . . .	18
V. CONCLUSIONS . . . . .	20

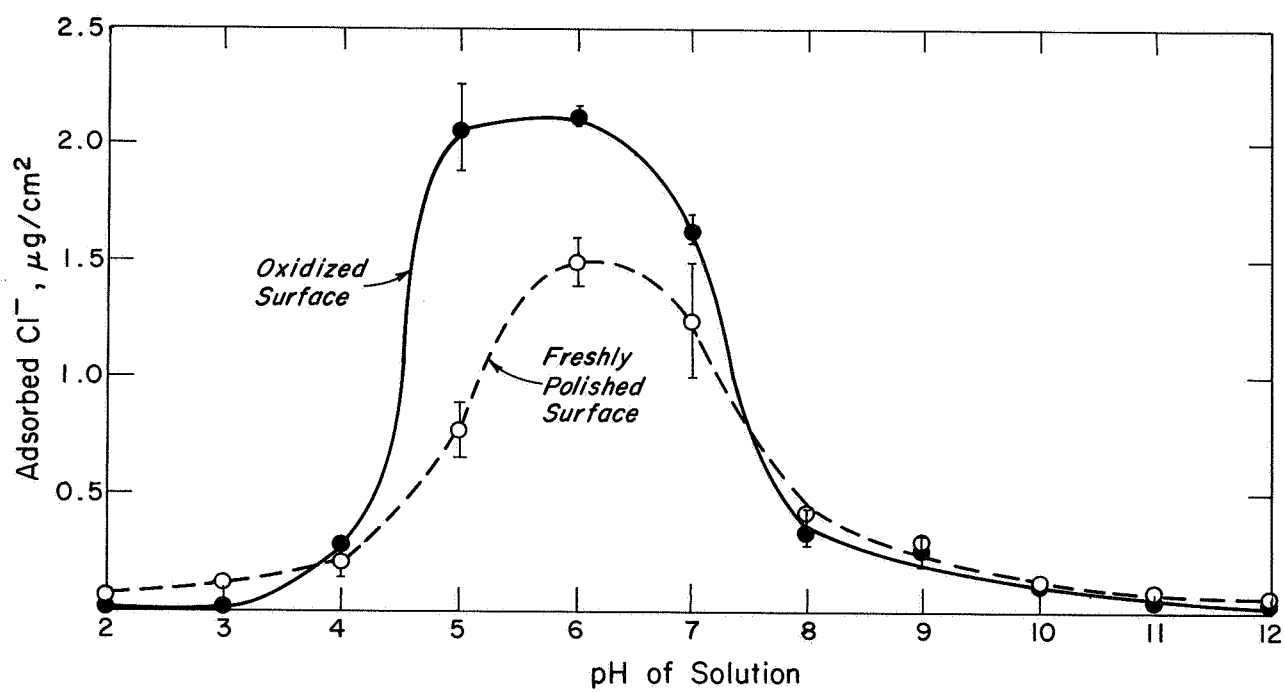


FIG. 1 EFFECT OF pH ON ADSORPTION OF  $\text{Cl}^-$  BY Ti-8Al-1Mo-1V IN NaCl SOLUTIONS <sup>(7)</sup>

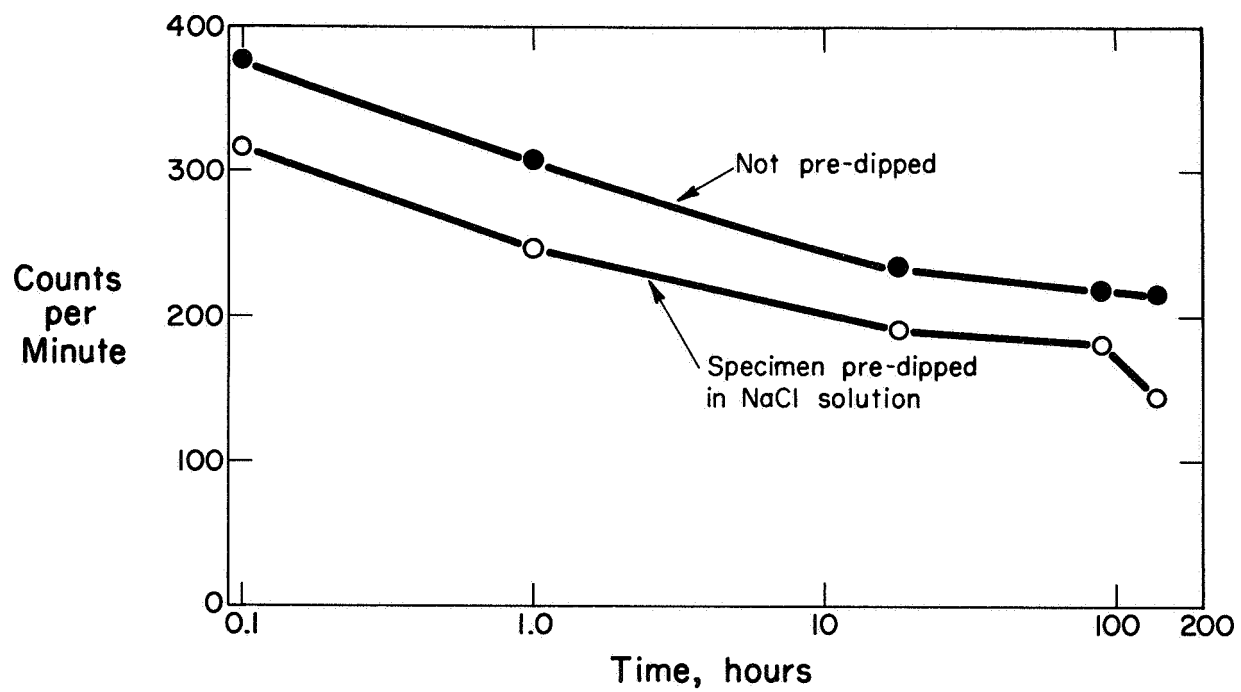


FIG. 2 RADIOTRACER EVIDENCE OF ADSORBED MOISTURE (OR  $^3\text{H}_2\text{O}$ ) ON Ti-8Al-1Mo-1V AT ROOM TEMPERATURE



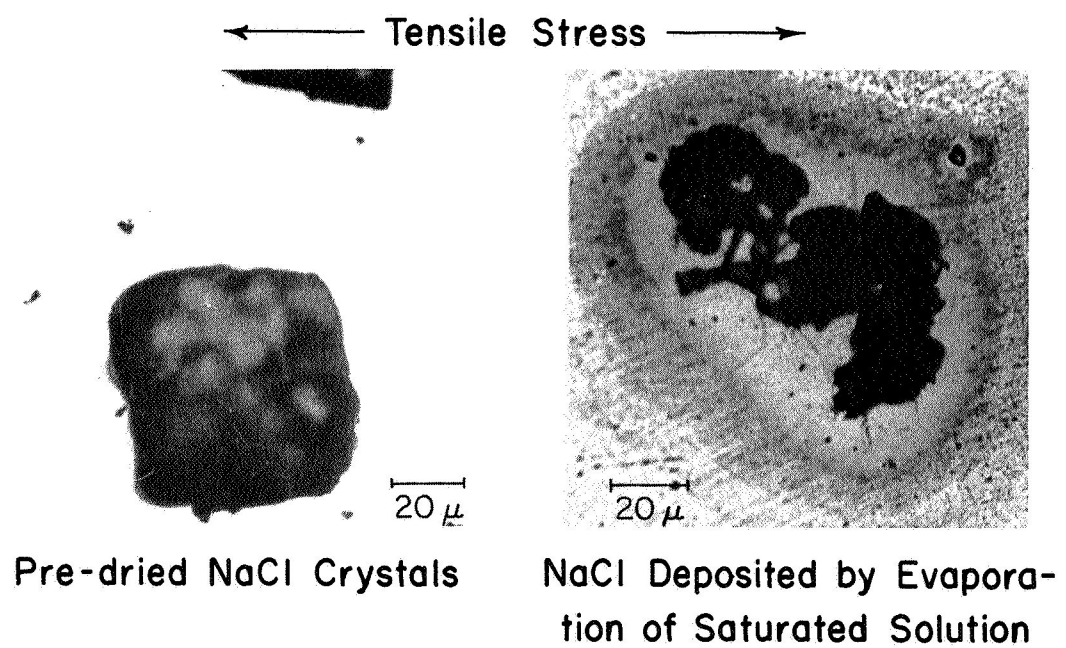


FIG. 3 EFFECT OF MOISTURE ON NaCl CRACKING OF Ti-8Al-1Mo-1V AT 650°F <sup>(7)</sup>  
(Specimen was exposed 90 minutes)

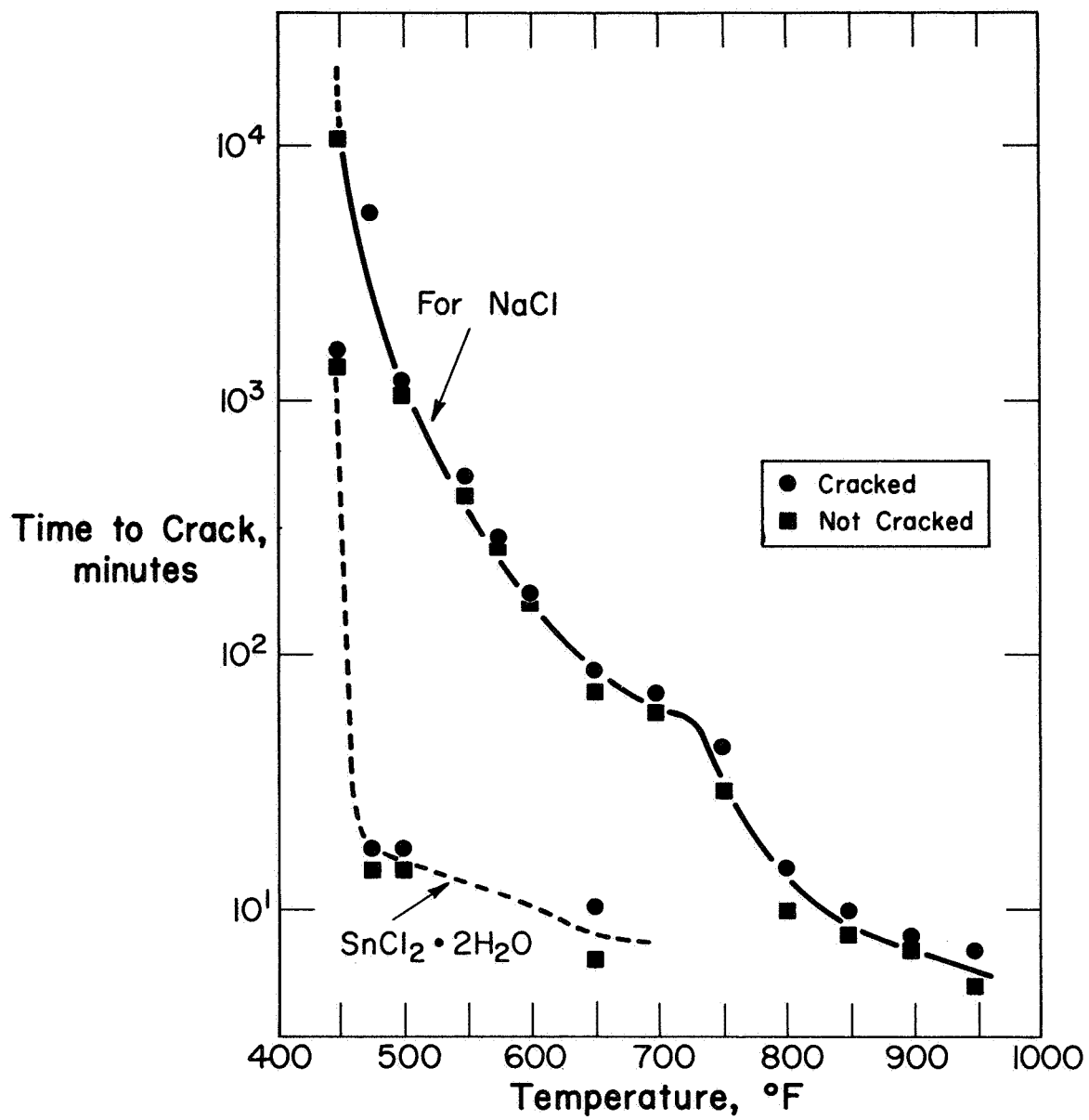
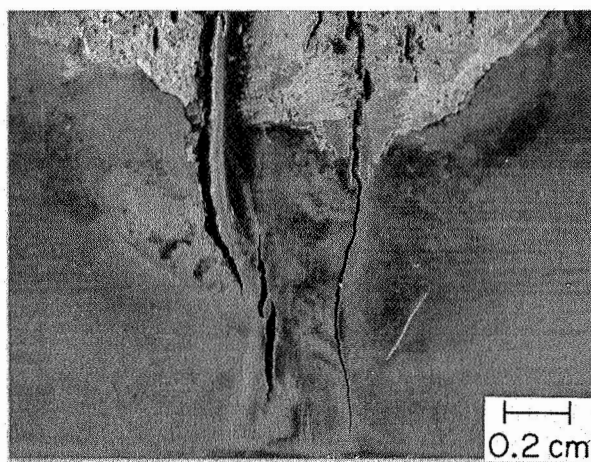
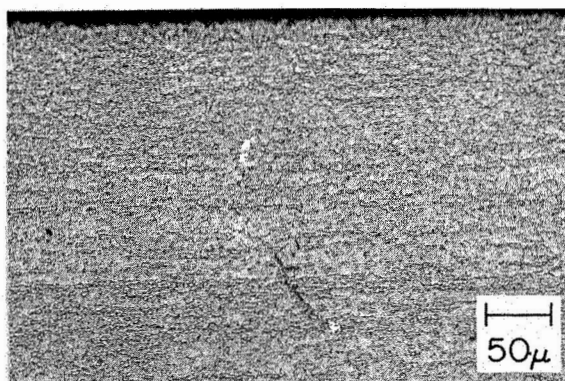


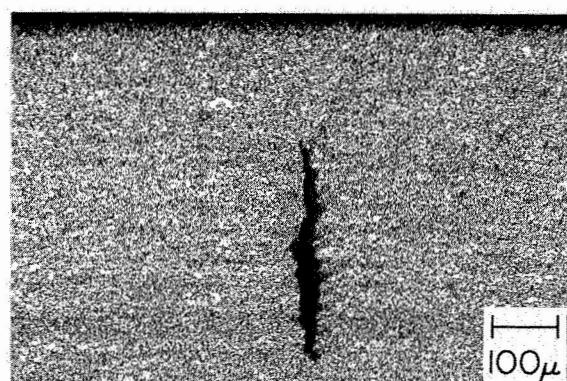
FIG. 4 EFFECTS OF SALT COMPOSITION AND TEMPERATURE ON TIME TO INITIATE CRACKING OF Ti-8Al-1Mo-1V



Top surface of specimen



Edge section



Edge section

FIG. 5 "TUNNELING" OF  $\text{SnCl}_2$ -INDUCED CRACKS IN Ti-8Al-1Mo-1V  
(Specimen was exposed at 650°F for 10 min.)

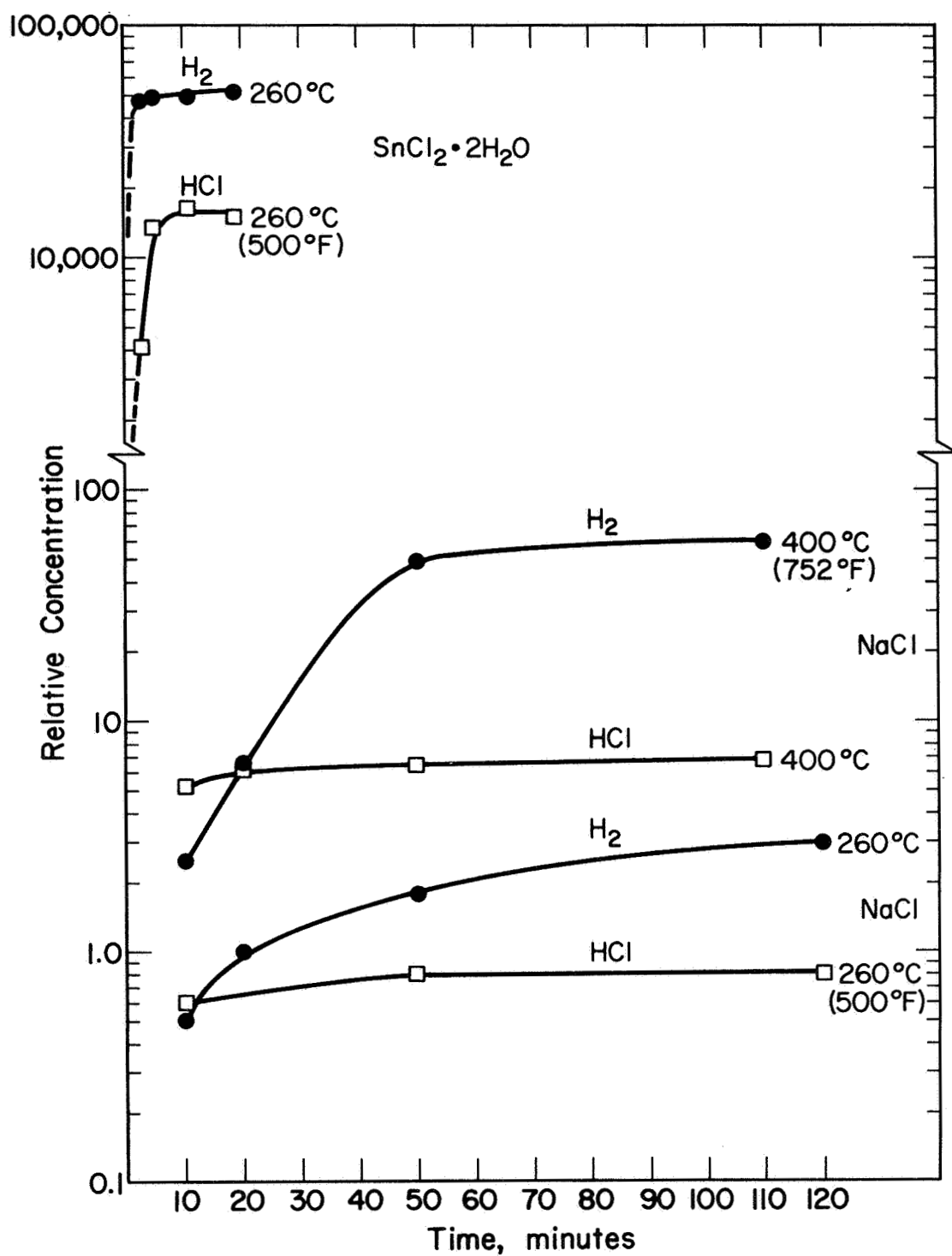


FIG. 6 EVOLUTION OF  $H_2$  AND  $HCl$  DURING HOT SALT CORROSION OF  $Ti-8Al-1Mo-1V$

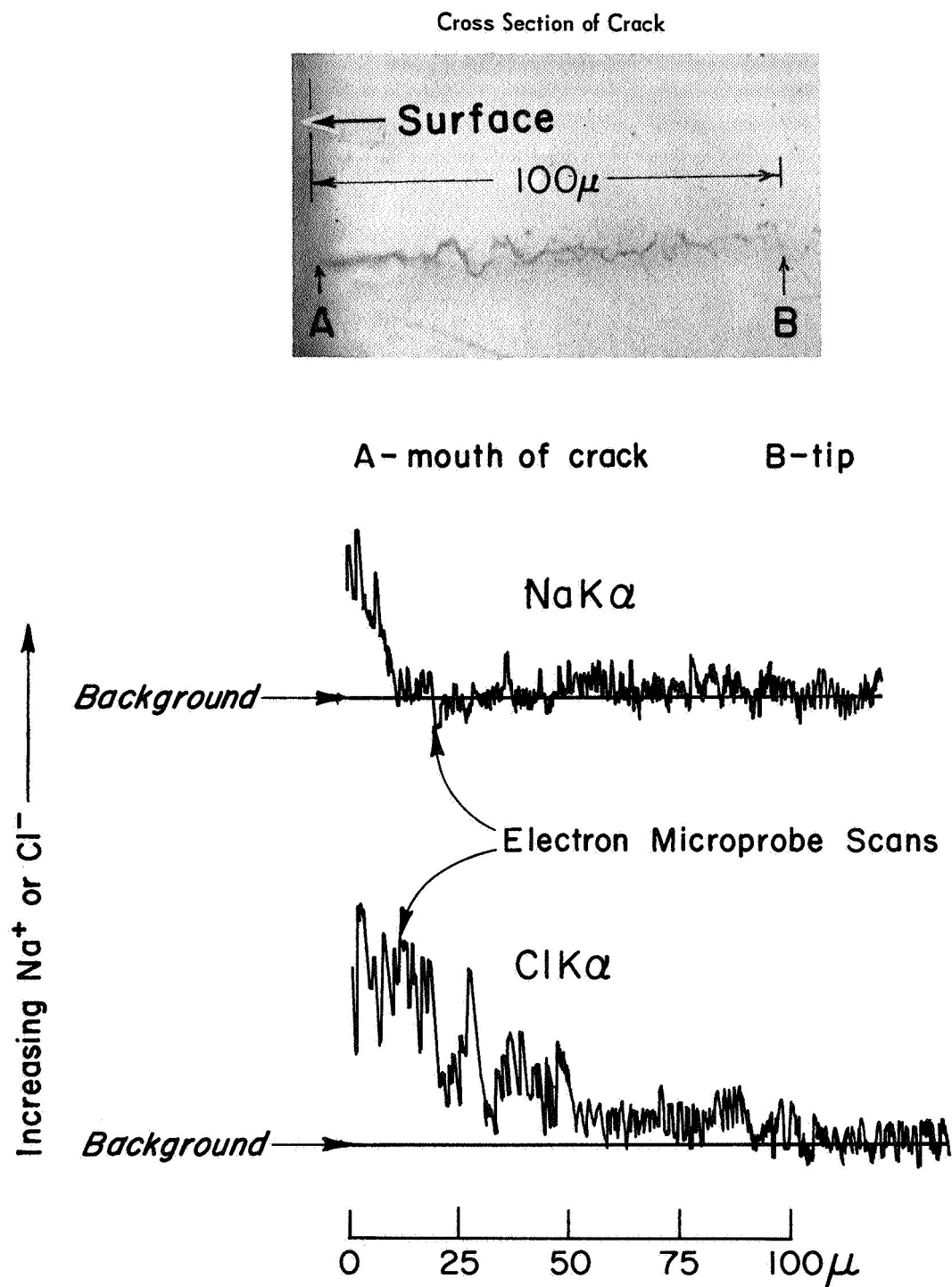


FIG. 7 ELECTRON MICROPROBE ANALYSES OF Na AND Cl IN HOT-SALT CRACK IN Ti-8Al-1Mo-1V <sup>(7)</sup>

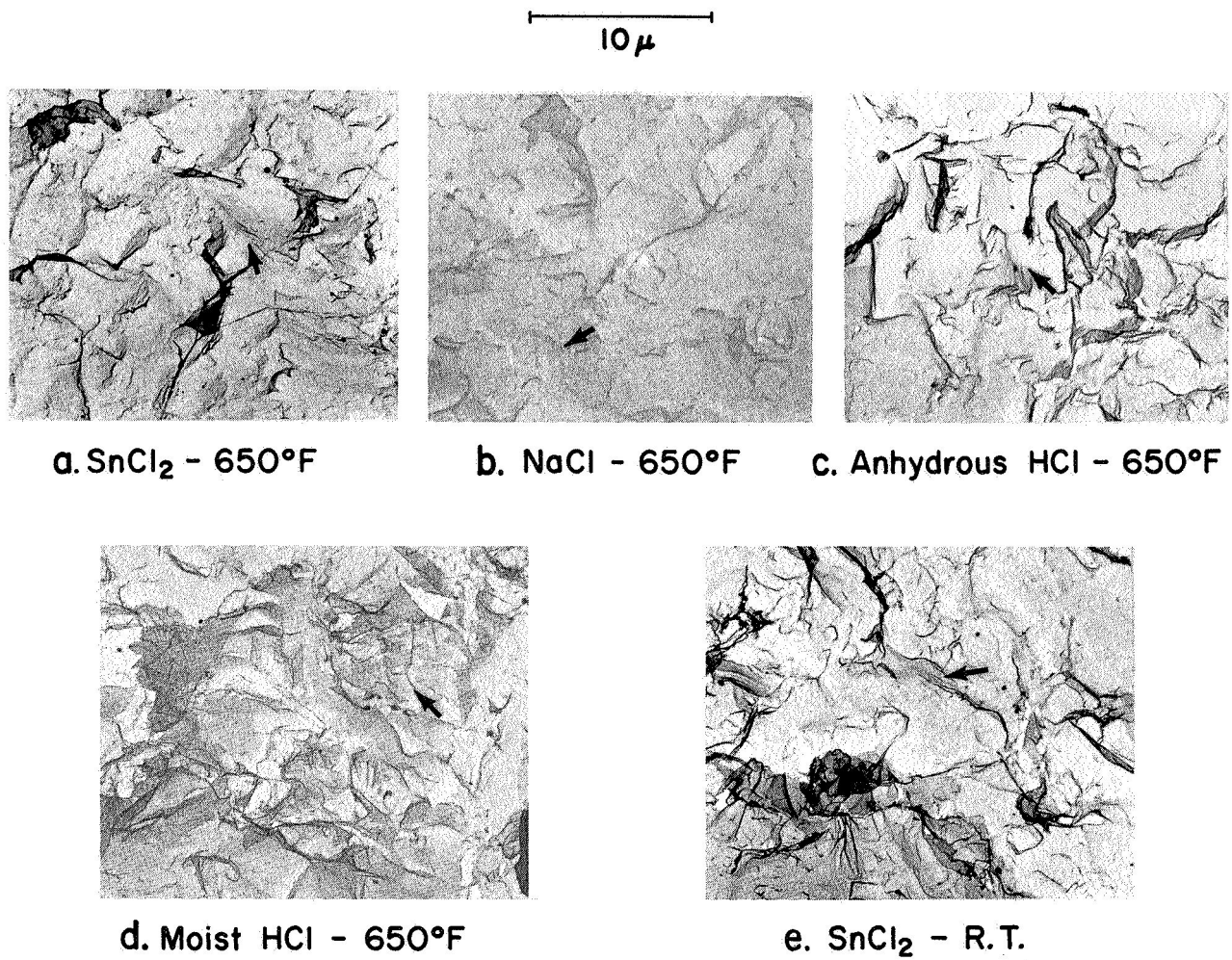
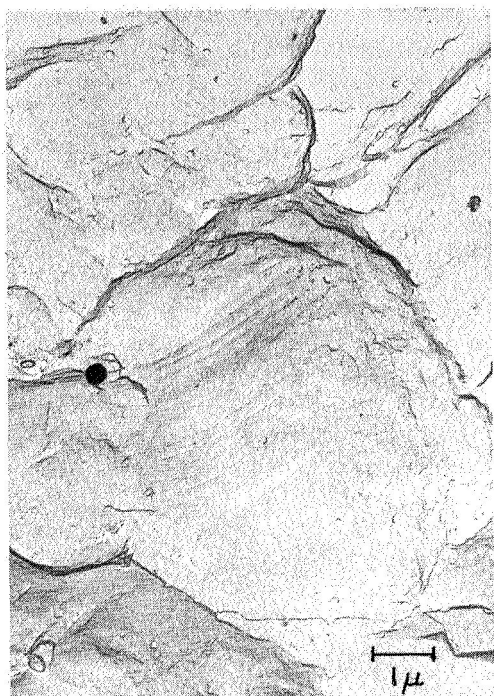
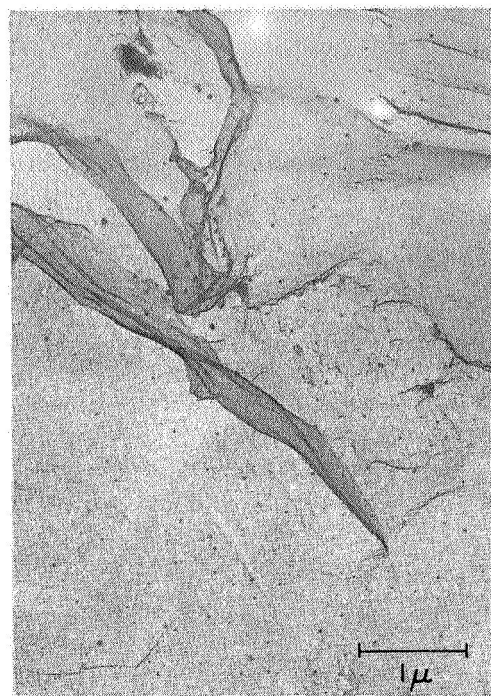


FIG. 8 TYPICAL FRACTOGRAPHS OF HOT-SALT CRACKS IN Ti-8Al-1Mo-1V



**NaCl - 650°F**

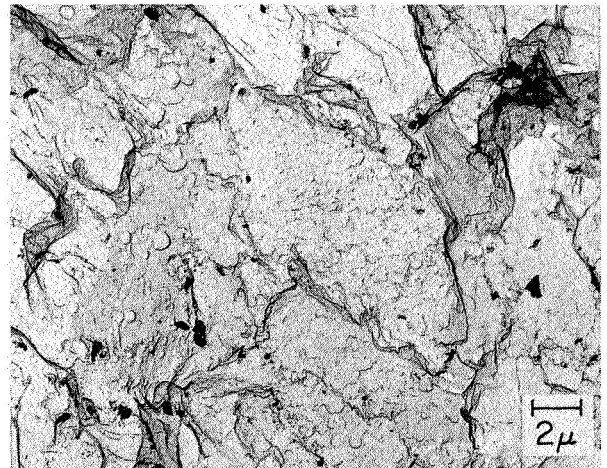


**Anhydrous HCl - 650°F**

**FIG. 9 FRACTOGRAPHS SHOWING EVIDENCE OF DISLOCATION MOVEMENT  
ACCOMPANYING FRACTURE DURING HOT-SALT CRACKING**



Anhydrous HCl at 650°F



SnCl<sub>2</sub> at 650°F

FIG. 10 FRACTOGRAPHS SHOWING EVIDENCE OF CORROSION OF FRACTURE FACES



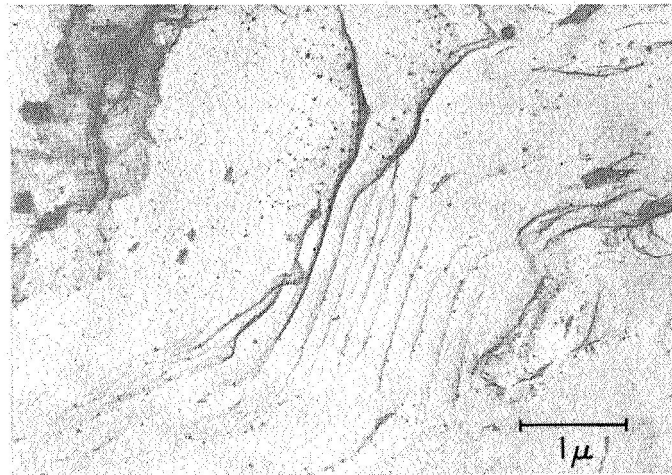


FIG. 11 FRACTOGRAPH SHOWING TYPICAL RIVER PATTERNS FOUND IN LIMITED REGIONS OF BOTH HOT-SALT AND HCl CRACKS